



**HAL**  
open science

## High-pressure Phase Transition and Properties of Cu<sub>3</sub>N: An Experimental and Theoretical Study

Aron Wosylus, Ulrich Schwarz, Lev Akselrud, Matt Tucker, Michael Hanfland,  
Rabia Kaneez, Christine Kuntscher, Jörg von Appen, Richard Dronskowski,  
Dieter Rau, et al.

► **To cite this version:**

Aron Wosylus, Ulrich Schwarz, Lev Akselrud, Matt Tucker, Michael Hanfland, et al.. High-pressure Phase Transition and Properties of Cu<sub>3</sub>N: An Experimental and Theoretical Study. *Journal of Inorganic and General Chemistry / Zeitschrift für anorganische und allgemeine Chemie*, 2009, 635 (12), pp.1959. 10.1002/zaac.200900369 . hal-00514959

**HAL Id: hal-00514959**

**<https://hal.science/hal-00514959>**

Submitted on 4 Sep 2010

**HAL** is a multi-disciplinary open access archive for the deposit and dissemination of scientific research documents, whether they are published or not. The documents may come from teaching and research institutions in France or abroad, or from public or private research centers.

L'archive ouverte pluridisciplinaire **HAL**, est destinée au dépôt et à la diffusion de documents scientifiques de niveau recherche, publiés ou non, émanant des établissements d'enseignement et de recherche français ou étrangers, des laboratoires publics ou privés.



## High-pressure Phase Transition and Properties of $\text{Cu}_3\text{N}$ : An Experimental and Theoretical Study

Journal:	<i>Zeitschrift für Anorganische und Allgemeine Chemie</i>
Manuscript ID:	zaac.200900369.R1
Wiley - Manuscript type:	Article
Date Submitted by the Author:	11-Aug-2009
Complete List of Authors:	<p>Wosylus, Aron; MPI-CPFS          Schwarz, Ulrich; MPI-CPFS          Akselrud, Lev; MPI-CPFS          Tucker, Matt; Rutherford Appleton Laboratory          Hanfland, Michael; ESRF          Kaneez, Rabia; Universität Augsburg, Institut für Physik          Kuntscher, Christine; Universität Augsburg, Institut für Physik          von Appen, Jörg; RWTH Aachen University, Institute of Inorganic          Chemistry          Dronskowski, Richard; RWTH Aachen University, Institute of          Inorganic Chemistry          Rau, Dieter; Universität Stuttgart, Institut für Anorganische Chemie          Niewa, Rainer; Universität Stuttgart, Institut für Anorganische          Chemie</p>
Keywords:	high pressure, nitride, copper, phase transition, semiconductor-metal transition



## ARTICLE

DOI: 10.1002/zaac.200((will be filled in by the editorial staff))

## High-pressure Phase Transition and Properties of Cu<sub>3</sub>N: An Experimental and Theoretical Study

Aron Wosylus,<sup>[a]</sup> Ulrich Schwarz,<sup>[a]</sup> Lev Akselrud,<sup>[a]</sup> Matt G. Tucker,<sup>[b]</sup> Michael Hanfland,<sup>[c]</sup>  
Kaneez Rabia,<sup>[d]</sup> Christine Kuntscher,<sup>[d]</sup> Jörg von Appen,<sup>[e]</sup> Richard Dronskowski,<sup>[e]</sup> Dieter Rau,<sup>[f]</sup>  
and Rainer Niewa,<sup>\*[f]</sup>

*Dedicated to Prof. Dr. Martin Jansen on the Occasion of his 65<sup>th</sup> birthday*

**Keywords:** High-pressure chemistry, Copper, Nitride, Electronic structure calculations

*In-situ* X-ray and neutron diffraction investigations on Cu<sub>3</sub>N indicate the onset of a high-pressure phase transition at about 5 GPa. The tetragonal cell parameters of the high-pressure phase reveal a discontinuous volume decrease of about 20 %. The phase transition is reversible, with a hysteresis of about 2 GPa. Subsequent *ex-situ* investigations in a multi-anvil press evidence a reversible re-formation of ambient pressure Cu<sub>3</sub>N from XRD patterns. The structure refinement with N atoms disordered in distorted octahedral voids of a tetragonal body-centered Cu-substructure leads to an occupation of approximately 1/3 and thus to a composition of Cu<sub>3</sub>N<sub>1.0(1)</sub>. Optical absorption measurements (IR-VIS) up to 10 GPa indicate a semiconductor–metal transition.

Density-functional based total energy calculations concerning the proposed high-pressure phase of Cu<sub>3</sub>N support strongly the experimental findings of a pressures-induced phase transition above 6 GPa to a structure with a Cu tetragonal body-centered sublattice and nitrogen atoms in distorted octahedral voids. However, the calculations identify a need for an ordered alternative to provide the tetragonal distortion within the range of the observed *c/a*-ratio. The resulting lattice parameters and the transition pressure fit with the measured data. For the case of an ordered occupation of the Cu *bct* octahedral voids, all observed properties are in good agreement with the calculations.

\* Institut für Anorganische Chemie, Universität Stuttgart,  
Pfaffenwaldring 55, 70569 Stuttgart, Germany  
Fax: ++49(0)711 / 685 64241  
E-mail: rainer.niewa@iac.uni-stuttgart.de

[a] Max-Planck-Institut für Chemische Physik fester Stoffe,  
Nöthnitzer Straße 40, 01187 Dresden, Germany

[b] Rutherford Appleton Laboratory, ISIS Facility, Didcot OX11  
0QX, Oxon, U.K

[c] European Synchrotron Radiation Facility, 38043 Grenoble,  
France

[d] Lehrstuhl für Experimentalphysik II, Institut für Physik,  
Universität Augsburg, Universitätsstraße 1, 86159 Augsburg,  
Germany

[e] Institute of Inorganic Chemistry at RWTH Aachen  
University, Landoltweg 1, 52074 Aachen, Germany

[f] Institut für Anorganische Chemie, Universität Stuttgart,  
Pfaffenwaldring 55, 70569 Stuttgart, Germany

semiconductor–metal transition. A very detailed work of Jansen et al. [4] recently investigated many promising high-pressure structure candidates by means of electronic structure calculations. The most promising has been identified to be the Li<sub>3</sub>P structure type, the K<sub>3</sub>N type, and the UO<sub>3</sub> type with transition pressures between 25 and 35 GPa. Contrary to this work, a second theoretical contribution [5] suggested the Cu<sub>3</sub>Au structure type for HP-Cu<sub>3</sub>N with a transition pressure of 17 GPa. However, so far reliable experimental high-pressure structure data are not available. Recently, independent from the investigations presented here, the electrical resistivity of Cu<sub>3</sub>N was studied in dependence of pressure, resulting in a likely metallization above about 5 GPa [6, 7].

### Results and Discussion

In a first series of experiments, Cu<sub>3</sub>N was treated at high pressures and high temperatures up to  $P = 9$  GPa and  $T = 500(80)$  K in a Walker type module before temperature quenching and pressure release. Analyses of the experiments reveal that the transformation products depend critically on the experimental conditions: We observed either the normal pressure modification of copper nitride (LP-Cu<sub>3</sub>N) or copper metal intermixed with copper nitride. The recovered ambient pressure modification of Cu<sub>3</sub>N exhibits a significantly increased full width at half maximum of the diffraction lines which is in accordance with a reversible phase transition. Figure 2 shows a comparison of diffraction patterns of LP-Cu<sub>3</sub>N before and after a pressure experiment. The formation of Cu metal in some experiments is attributed

### Introduction

The semiconducting nitride Cu<sub>3</sub>N was first synthesized by Juza and Hahn in 1938 and is since known to crystallize in a so-called inverse ReO<sub>3</sub> crystal structure (Fig. 1), an exclusive situation for binary transition metal nitrides [1, 2]. Due to its low density caused by large open voids this type of atomic arrangement qualifies as a likely candidate for pressure-induced phase transitions. This assumption is also supported by the experimental observation of a structural change of the parent compound ReO<sub>3</sub> upon compression [3]. Moreover, the results of electronic structure calculations [4, 5] indicate a pressure-induced phase transition of ReO<sub>3</sub>-type Cu<sub>3</sub>N between 15 GPa and 35 GPa probably subsequent to a

to pressure gradients and shear stresses in the octahedra and the metastable nature of  $\text{Cu}_3\text{N}$ .

*In-situ* X-ray diffraction investigations, carried out in a diamond anvil cell with a methanol-ethanol mixture (4:1), Ar and He as pressure-transmitting media, indicate stability of the cubic low-pressure modification below 5(1) GPa. In direction of increasing pressures, the onset of the transformation into a high-pressure phase (HP- $\text{Cu}_3\text{N}$ ) is observed around 5 GPa (Figs. 3 and 4). The evaluation of the diffraction patterns in direction of increasing pressure (Figure 3) indicate a two-phase region, in which residual LP- $\text{Cu}_3\text{N}$  and the high-pressure phase coexist. The coexistence regime in experiments with alcohol mixtures as pressure medium is significantly smaller than with argon, which is attributed to a coupling of the stress-components to the phase transitions. The resulting overlap of unresolved reflections with diffraction angles of, e.g.  $2\theta = 10.8$  and  $12$  degrees, obscure the lattice parameters and thus the volume determination. Consequently, no structure refinements were performed between 4.5 and 8.7 GPa. According to the data with Ar as pressure medium the phase transition is reversible with a hysteresis of about 2 GPa. In accordance with this finding, *ex-situ* investigations in a multi-anvil press show re-formation of pure normal-pressure  $\text{Cu}_3\text{N}$  as revealed by X-ray powder diffraction patterns. Thus, the available experimental data are consistent with the assumption that the composition of the high-pressure phase corresponds to that of the low-pressure modification within the limits of experimental error.

The X-ray powder diffraction patterns at pressures above the structural phase transition differ significantly in runs with different pressure media (see Fig. 5). Thus, the discussion of structure models is based on the diffraction data measured with helium as pressure transmitter in direction of increasing pressures only, since He exhibits the smallest deviation from hydrostatic conditions. The intensity distribution of the HP-phase resembles roughly that of *fcc* copper, but splitting of the  $(200)_{fcc}$  and  $(220)_{fcc}$  reflections indicate a lower symmetry (see Fig. 3). Choosing the tetragonal subgroup  $I4/mmm$  ( $a \approx 260$  pm,  $c \approx 380$  pm) the most intense lines can be indexed satisfactory, especially at pressures exceeding 30 GPa. However, further peak splitting (especially of  $(220)_{fcc}$ ) and additional lines (at  $2\theta \approx 6.4^\circ$  and  $2\theta \approx 11.8^\circ$ ) evidence an even lower symmetry (or a hitherto unidentified second phase). Aiming to describe these additional lines, a model in orthorhombic space group  $Immm$  was chosen. Additionally, the observed peak broadening was described by a phenomenological model which takes into account the effects of strain [8]. At 10.5 GPa, the refinements yield a small, but significant deviation from tetragonal symmetry with  $a = 380.2(2)$  pm,  $b = 393.5(2)$  pm and  $c = 742.7(3)$  pm (see Fig. 6). The atomic volume of the orthorhombic  $Immm$  indexing differs by only 0.1 % from the tetragonal solution so that we take the higher symmetry data for the pressure-volume relation.

Intensity calculations indicate that the tetragonal partial structure of the high-pressure modification does not resemble any of the known modifications of the well-studied isotypic  $\text{ReO}_3$  or any of the favorable structure types considered in the previous structure predictions from electronic structure calculations [4, 5]. According to the X-ray diffraction data the copper substructure adopts a tetragonal body centered arrangement (Cu atoms occupying

position  $2b$  ( $0,0,1/2$ ) of  $I4/mmm$ ) which resembles the motif of the indium metal structure, but the nitrogen positions could not be reliably located by means of the X-ray diffraction experiments due the disadvantageous ratio of the X-ray scattering factors (Table 1).

Aiming to locate the nitrogen atoms in the crystal structure, we performed high-pressure neutron diffraction experiments since copper and nitrogen have very similar neutron scattering factors ( $b(\text{Cu}) = 7.9$  fm,  $b(\text{N}) = 9.4$  fm). The pressure-induced volume changes correspond to the data obtained from X-ray diffraction. Figure 7 shows neutron diffraction patterns at different pressures. Next to reflections arising from  $\text{Cu}_3\text{N}$ , reflections of Pb (pressure marker), WC (anvil material) and Ni (crucible material) are visible. The phase transition of  $\text{Cu}_3\text{N}$  is clearly indicated by the disappearance of reflections of low-pressure copper nitride. The reflections due to high-pressure copper nitride only slowly grow from the background on increasing pressure and stay broad and weak. This fact is best seen from the reflections at TOF  $\approx 18$   $\mu\text{s}$ : For LP- $\text{Cu}_3\text{N}$  the (100) reflection presents as the strongest signal. At 6.9 GPa no trace of this reflection is left in the pattern. Within the experimental resolution the tetragonal substructure can clearly be confirmed, but due to the experimental conditions given by the high-pressure set-up (signal to noise ratio limited by the small sample volume, additional scattering contributions of container material, anvil and pressure marker) superstructure reflections are not detected in the neutron scattering data. The absence of extra reflections would indicate that under the pressure conditions of the neutron scattering experiment nitrogen atoms are randomly disordered in the overall crystal structure of the high-pressure phase. The structure refinement with nitrogen atoms disordered in the distorted octahedral voids of the tetragonal body-centered Cu-substructure leads to an occupation of 0.33(1) for the pattern at 8.2 GPa and by this in the description in space group  $I4/mmm$  (Table 1) to an unit cell content of  $\text{Cu}_2\text{N}_{0.66(1)}$ , which resembles the composition  $\text{Cu}_3\text{N}_{1.0(1)}$ . However, refinements of different patterns in the pressure range of about 8.2 – 9.5 GPa result in a site occupancy variation from 0.28 – 0.38, i.e., compositions in the range from  $\text{Cu}_3\text{N}_{0.84}$  to  $\text{Cu}_3\text{N}_{1.14}$ .

Figure 8 shows the average tetragonal arrangement. Interatomic distances  $d(\text{Cu}-\text{N})$  of  $^{4/3} \times 187.6(1)$  pm and  $^{2/3} \times 195.4(1)$  pm at 8.2 GPa are compatible with the value observed for the ambient pressure  $\text{ReO}_3$ -type structure with  $d(\text{Cu}-\text{N}) = 191$  pm [1, 2]. The complete structure model represents an elongated rocksalt structure with disordered defects in the anionic substructure. Thus, HP- $\text{Cu}_3\text{N}$  fits well into the majority of well-studied and technologically relevant binary transition metal nitrides in which nitrogen is located in octahedral voids. Moreover, a similar structure is known for the ambient temperature form of  $\theta\text{-Mn}_6\text{N}_{5+x}$  realizing a tetragonal defect rocksalt structure. The reason for the distortion in the Mn case is believed to be the antiferromagnetic order [9]. Similarly, for CrN the cubic rocksalt type structure at ambient temperature distorts to orthorhombic below the Néel temperature due to magnetic ordering [10]. Still, the absence of magnetic moments in copper nitride leaves the reason for the distortion in the title compound unknown. Parallel performed electronic structure optimizations with the disordered structure model for the high-pressure phase of  $\text{Cu}_3\text{N}$  relax with the  $c/a$  ratio of a cubic *fcc* lattice. This disagreement to the experimental data

can be taken as an indication for an ordered structural ground state, at least at the local level of several unit cell sized domains (see below).

A comparison of the unit cell volumes reveals that the structural transformation from the low-pressure into the high-pressure phase is associated with a discontinuous change of volume of about  $-20\%$ . However, consideration of a peculiar volume scatter in data with alcohol as pressure transmitting medium may allow for an alternative explanation involving a slight change of the chemical composition from  $\text{Cu}_3\text{N}$  to a nitrogen-rich phase. The subsequent production of elemental Cu might not be detectable in the products after pressure release with diffraction techniques and additionally be shaded by the occasional Cu formation due to decomposition of the metastable LP- $\text{Cu}_3\text{N}$  triggered by shear-forces. This and further open points are going to be addressed via electronic structure calculations.

The magnitude of the volume change associated with the phase transformation can be compared to an estimation based on an analysis of sphere packing. In the ambient-pressure phase of  $\text{Cu}_3\text{N}$  with linearly coordinated copper, the metal atoms adopt a defect variant of an *fcc* arrangement in which only  $75\%$  of the atomic positions are filled. The high-pressure modification adopting a body centered tetragonal copper arrangement can be described as a slightly distorted *fcc* pattern of metal atoms in which all positions are occupied. As a result, the packing density of the metal atoms is significantly increased and accounts surprisingly well for the experimentally observed volume change of  $-20\%$ .

A compressibility of  $B_0 = 114(2)$  GPa for LP- $\text{Cu}_3\text{N}$  results from application of a least squares refinement of a linear equation to the experimental data ( $V_0 = 55.48(2) \cdot 10^6 \text{ pm}^3$ ). This bulk modulus is surprisingly similar to the value for the isotopic  $\text{ReO}_3$  phase (100 GPa [11]) and to a value obtained from electronic structure calculations (115.2 GPa) [12]. An increased resistance of the linear arrangement at  $\text{Cu}^1$  against bending deformation is indicated by the different structural high-pressure behaviour of  $\text{Cu}_3\text{N}$  and isostructural  $\text{ReO}_3$ , explaining the absence of distortion variants due to octahedra rotation for the nitride. The linear thermal expansion of LP- $\text{Cu}_3\text{N}$  below ambient temperatures is in the normal range for semiconductors, and also indirectly supports this view. For comparison, the linear thermal expansion of  $\text{ReO}_3$  has a small positive or even negative value depending on temperature due to intensifying thermal rotation of the  $\text{ReO}_{6/2}$  octahedra, *i.e.*, smaller angles at the bridging oxygen atoms with increasing temperatures [13].

Concomitant with the discontinuous volume change, dramatic changes occur in the electronic properties, as indicated by the pressure-dependent optical response. The pressure-dependent transmission and absorption spectra in the infrared and visible frequency range are depicted in Fig. 9. At the lowest applied pressure (1.0 GPa) we observe a strong increase of the absorption (indicated by an arrow) at around  $8000 \text{ cm}^{-1}$  (1 eV) due to excitations across the band gap. The location of the absorption edge is in good agreement with the calculated band gap earlier estimated from electronic structure calculations (0.9 eV) [14]. For pressures above  $\sim 4$  GPa the absorption strongly increases in

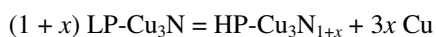
the infrared frequency range, which can be attributed to additional electronic states close to the Fermi level induced by pressure. Above  $\sim 7$  GPa the changes with increasing pressure are small and the absorption spectrum is almost flat. These findings suggest that  $\text{Cu}_3\text{N}$  undergoes a transition from a semiconductor to a metal induced in the pressure range  $4 - 7$  GPa. A similar pressure range for the pressure-induced semiconductor-metal transition was earlier observed in electrical resistivity measurements in diamond anvil cells [6, 7]. Upon pressure release the initial low absorption level in the infrared range is not recovered, as illustrated by the spectrum for 1.8 GPa (see Fig. 9 b); this finding is in agreement with the hysteresis observed in our pressure-dependent diffraction measurements and with the pressure-dependent dc transport [7].

As a first step in electronic structure calculations, and a quality assurance for the selected method, we reproduced the experimentally obtained properties for  $\text{ReO}_3$  type LP- $\text{Cu}_3\text{N}$ . For this purpose, the optimized geometry and total energy was calculated by fully relaxing the structure. The obtained lattice parameter of the LP- $\text{Cu}_3\text{N}$  (Table 2) fits well with the experimental data. It is slightly overestimated (0.8 %) by the calculation, a typical peculiarity of the GGA approximation. A comparison with the total energy of the elements ( $3 \text{ Cu} + \frac{1}{2} \text{ N}_2$ ) demonstrates the known metastability of LP- $\text{Cu}_3\text{N}$ . The calculated heat of formation at 0 Kelvin yields to  $\Delta H_f = 1.21$  eV per formula unit. Subsequently, we developed the energy-volume curve (Figure 10, top) by fitting the 15  $E(V)$  data points with the Murnaghan equation of state.

Next, total energy calculations of the experimentally suggested structure with the composition  $\text{Cu}_3\text{N}$  were performed. Because of the proposed disordered nitrogen atoms a supercell technique was employed ( $3 \times 3 \times 3$  unit cells containing 54 copper atoms and 18 nitrogen atoms). 20 different of such cells were created by randomly occupying 18 of the 54 octahedral voids with nitrogen. All structures have been automatically relaxed under the constraint of fixed atom positions (else the structure would break down, because supercells are, unfortunately, far away from a statistically occupied crystal). The variation in total energy within the 20 structures is only  $1.7\%$ , in volume it is less than  $1\%$ . Due to these results, we reason that the supercell is large enough to approximately represent the entire crystal. The average lattice parameters for the conventional unit cell at zero pressure are  $a = 2.81 \text{ \AA}$  and  $c = 3.95 \text{ \AA}$ . The phase transition enthalpy from the  $\text{ReO}_3$ -type to the most stable nitrogen distribution amounts to  $0.87$  eV per formula unit, the volume of the potential high-pressure phase is about  $18\%$  smaller. This volume decrease in combination with the not too large endothermic enthalpy indicates a possible high-pressure transition. Namely, for the approximation of same bulk moduli one can calculate a zeroth order transition pressure of  $p_{\text{trans}} = -\Delta E/\Delta V \approx 11$  GPa. Hence, and to make a comparison with the experimental results possible (that are only available at high pressures), we investigated the compounds' properties under pressure as described above and obtained the  $E-V$  and the  $\Delta H-p$  curves. Both are displayed in Fig. 10. Some further physical properties of the LP- $\text{Cu}_3\text{N}$  and the proposed high-pressure phase are listed in Table 2. The energy-volume diagram shows the smaller equilibrium volume and higher energy of the high-pressure phase. As a consequence, at pressures above 16 GPa it

becomes thermodynamically stable, as the enthalpy–pressure diagram evidences. At the experimentally detected transition pressure the compound is 0.39 eV less stable than LP-Cu<sub>3</sub>N (Table 2), its volume is about 7 % larger than the experimentally obtained one. However, most profound is the deviation of the *c/a*-ratio. All 20 statistically occupied structures relax from the experimentally start value of *c/a* = 1.50 to one between 1.37 and 1.43 in the course of calculation. Even at high pressures this ratio remains. Conspicuously, the average ratio has been calculated to 1.41  $\approx \sqrt{2}$ . A body centered tetragonal cell with *c/a* =  $\sqrt{2}$  means nothing else but a face centered cubic (*fcc*) cell. With the aim to audit this result and exclude errors due to too small supercells, we repeated the calculation with a larger 5 × 5 × 3 supercell containing 150 copper and 50 nitrogen atoms. The *c/a*-ratio decreased again from the start value 1.50 to 1.417 and confirmed our previous result. The thought, that *fcc* copper incorporates nitrogen statistically onto the octahedral voids and remains *fcc*, is not farfetched. As was already commented in the discussion of the experimental results the reason for the tetragonal distortion is unknown. From the theoretical point of view, the reason does not exist and the structure relaxes into the more stable cubic one. Nonetheless, the statistical occupied *fcc* type Cu<sub>3</sub>N is more stable than all other yet considered alternatives.

The finding of elemental copper produced in few pressure experiments, lead to the speculation about a slight change in chemical composition. Possibly this different composition is responsible for the tetragonal distortion. We took this into account by creating each 10 of 3 × 3 × 3 supercells with the compositions Cu<sub>54</sub>N<sub>19</sub>, Cu<sub>54</sub>N<sub>20</sub>, and Cu<sub>54</sub>N<sub>21</sub> and an initial *c/a* value of 1.50. All compounds have been relaxed with respect to the volume and the cell geometry. The results for the *c/a*-ratio and the theoretical reaction enthalpies for



are shown in Figure 11. The nitrogen content seems to have no influence on the *c/a*-ratio. The values for all compositions relax downwards and are finally distributed around  $\sqrt{2}$  again. Also, the reaction enthalpies give no hint, that a disproportionation into elemental copper and a nitrogen richer phase is lucrative, either.

With the purpose to simulate the actual experimentally identified structure, i.e. a relaxed groundstate whose properties fit with the experimental ones, we allowed a more regular arrangement of the nitrogen atoms. A representative compound AB<sub>3</sub>, that crystallizes in a *bct* sublattice of B and the octahedral voids filled with A atoms, does, to the best of our knowledge, not exist. Hence, we occupied 2 × 2 × 2 (16 Cu atoms) and 3 × 3 × 3 (54 Cu atoms) copper *bct* sublattices with 6 respectively 18 nitrogen atoms in a way, that the compound will presumably retain its dilation in *c*-direction. The latter supercell represents the suggested composition Cu<sub>3</sub>N, whereas the smaller supercell has a nitrogen content of 0.375 (Cu<sub>3</sub>N<sub>1,125</sub>). We found just a few unit cells that satisfied the requirements of both a tetragonal symmetry and the approximated experimentally detected ratio of the lattice parameters (Figs. 12 and 13). The data of the most promising structure for each composition are shown in Table 3, the unit cells are presented in Figure 14. The formulas document the resulting size of the unit cell (caused by symmetry reduction in the case of Cu<sub>12</sub>N<sub>4</sub>). In order to avoid confusion between the statistical and ordered

structures we retain this labeling for the following. As one can read from Table 3, both the Cu<sub>16</sub>N<sub>6</sub> and the Cu<sub>12</sub>N<sub>4</sub> remain tetragonal during the relaxation with an optimized *c/a*-ratio of 1.51 respectively 1.49. At zero pressure a transition from the low-pressure ReO<sub>3</sub> type under conservation of the composition would require 0.39 eV, a disproportionation into Cu and Cu<sub>16</sub>N<sub>6</sub> 0.36 eV. That means, that this ordered tetragonal compounds are about 0.5 eV per formula unit Cu<sub>3</sub>N more stable than the most stable calculated statistical and hence cubic structure. The subsequent high-pressure examination produced results that are shown in Figure 14. Some more detailed properties at the experimentally described 8.2 GPa are shown for a comparison in Table 3, too. Both ordered phases become more stable with respect to the LP-Cu<sub>3</sub>N at about 6 GPa, the nitrogen-richer phase is a little bit more stable over the total pressure range. However, the enthalpy difference is at each pressure just 0.03 – 0.04 eV, too little for a substantiated interpretation. The *c/a*-ratio of the Cu<sub>16</sub>N<sub>6</sub> amounts 1.50 at pressures around 8 GPa and agrees with the experimentally found value in X-ray diffraction at 7.8 GPa, for Cu<sub>12</sub>N<sub>4</sub> it decreases under pressure and agrees at ca. 8 GPa with the experimental data from neutron diffraction at 8.2 GPa. The volume decrease caused by the phase change has been measured to be approximately 20 %, for Cu<sub>12</sub>N<sub>4</sub>/Cu<sub>16</sub>N<sub>6</sub> it amounts to about 18 % and 16 %, respectively. The corresponding lattice parameters are 2 % overestimated, in good accordance with the expected overestimation due to the GGA approximation. However, considering both unit cells, one finds a chemical counterintuitive situation. For the composition Cu<sub>16</sub>N<sub>6</sub>, the most likely coordination for the metal would be square-planar for two Cu<sup>2+</sup> and linear for 14 Cu<sup>+</sup>. But we find also T-shaped coordination as well as nitrogen-uncoordinated copper. For Cu<sub>12</sub>N<sub>4</sub>, a regular linear coordination of the copper atoms would be intuitive, but this structure suggestion has beside this coordination numbers of 0, 1, and 3. This situation is implausible, albeit it is to consider, that the proposed statistical occupation will offer all kinds of these coordination environments, too. In the sum, due to the tremendous number of possibilities to distribute the nitrogen atoms in an ordered way, and furthermore the unusual coordination of copper in this two suggestions, we don't want to claim, that one of these is the true structure of high-pressure Cu<sub>3</sub>N. At this point, let us recall the above depicted irregularities detected in some experiments. One possibility, that would explain all of these facts, is the formation of different phases (potentially due to small local pressure variation) side by side. It was already mentioned that a production of Cu metal can be attributed to pressure gradients and shear stresses. The very small enthalpy differences between the different ordered phases support this idea. Additionally, this would explain that an ordering of nitrogen cannot be found in the diffraction data. But these considerations should just be taken as a careful guess to bring together the experimental and theoretical results. However, all theoretical findings in this work indicate, that a kind of nitrogen ordering exists in HP-Cu<sub>3</sub>N. For a final clarification further work is required.

Figure 1. Crystal structure of the low-pressure modification of  $\text{Cu}_3\text{N}$  ( $\text{ReO}_3$  type). White spheres correspond to copper atoms, the vertex-sharing coordination octahedra surrounding nitrogen are indicated.

Figure 2. XRD pattern of LP- $\text{Cu}_3\text{N}$  before (bottom line) and after (top line) a pressure treatment in the multi-anvil cell at about 9 GPa ( $\text{Co-K}\alpha_1$  radiation).

Figure 3. X-ray powder diffraction pattern ( $\lambda = 41.3082$  pm) collected on increasing pressure with helium as pressure medium. The positions of the diffraction lines are marked on the bottom and top for LP- $\text{Cu}_3\text{N}$  and HP- $\text{Cu}_3\text{N}$  respectively. Stars mark the strongest reflections of the pressure medium.

Figure 4. Change of the atomic volume of  $\text{Cu}_3\text{N}$  with increasing pressure (data with He as pressure transmission medium only, for hysteresis see main text). The insert shows the change of  $c/a$  for the high-pressure phase. The line represents the quotient of the fitted equation of states for the lattice parameters.

Figure 5. Comparison of X-ray powder diffraction data of HP- $\text{Cu}_3\text{N}$  ( $\lambda \approx 41$  pm) recorded in runs with different pressure media (methanol : ethanol = 4:1). The diagrams indicate intensity changes which are attributed to different stress conditions and the resulting differences for the formation of HP- $\text{Cu}_3\text{N}$ . Please note the superstructure reflections at approximately  $6.4^\circ$  and  $11.8^\circ$ .

Figure 6. Diffraction pattern and difference between observed and calculated intensities of HP- $\text{Cu}_3\text{N}$  in the orthorhombic space group  $Immm$  using a phenomenological strain model. The insert shows a magnification of the low angle part of the diffraction pattern including weak unindexed reflections.

Figure 7. Neutron diffraction patterns (TOF in  $\mu\text{s}$ ) of  $\text{Cu}_3\text{N}$  measured at different pressures. N, P and W assign prominent reflections of Ni crucible, lead pressure indicator and WC anvils, respectively.

Figure 8. Average tetragonal crystal structure of the high-pressure modification of  $\text{Cu}_3\text{N}$  from experimental data. White spheres correspond to copper atoms. Nitrogen positions (dark spheres) are only occupied to  $1/3^{\text{rd}}$ .

Figure 9. (a) Transmission  $T(\omega) = I_s(\omega)/I_i(\omega)$  (see text for definitions) of  $\text{Cu}_3\text{N}$  at ambient temperature as a function of pressure and (b) the corresponding absorption  $A = \log_{10}(1/T)$  as a function of pressure. The arrow in (b) indicates the frequency position of the absorption edge.

Figure 10: Energy–volume- (top) and enthalpy–pressure-diagram (bottom) of the  $\text{ReO}_3$  type LP- $\text{Cu}_3\text{N}$  and the proposed high-pressure phase.

Figure 11: Tetragonal lattice parameter ratio  $c/a$  (top) and associated heat of formation (relative to low pressure  $\text{Cu}_3\text{N}$ ) per formula unit in dependence of the N content (bottom).

Figure 12:  $\Delta H$ – $p$  diagram of the nitrogen ordered phases  $\text{Cu}_{12}\text{N}_4$  and  $\text{Cu}_{16}\text{N}_6$  relatively to the low pressure  $\text{ReO}_3$ -type.

Figure 13:  $V$ – $p$  diagram of the nitrogen ordered phases  $\text{Cu}_{12}\text{N}_4$ ,  $\text{Cu}_{16}\text{N}_6$  and the low pressure  $\text{Cu}_3\text{N}$ .

Figure 14: Unit cells of the nitrogen-ordered structure suggestions  $\text{Cu}_{12}\text{N}_4$  (left) and  $\text{Cu}_{16}\text{N}_6$  (right). N = dark spheres, Cu = light spheres.

Table 1. Crystallographic data of  $\text{Cu}_3\text{N}$ .

X-ray diffraction data <sup>[a,b]</sup>	
Low-pressure phase	
Pressure / GPa	4.5
Space group	$Pm\bar{3}m$ (no. 221)
Lattice parameter / pm	376.52
Copper position	$1/2, 0, 0$
Nitrogen position	$0, 0, 0$
High-pressure phase	
X-ray diffraction data <sup>a</sup>	
Pressure / GPa	8.7
Space group	$I4/mmm$ (no. 139)
Lattice parameters $a$ / pm	265.88
$c$ / pm	394.69
Copper position	$0, 0, 0$
Neutron diffraction data <sup>[c]</sup>	
Pressure / GPa	8.2
Space group	$I4/mmm$ (no. 139)
Lattice parameters $a$ / pm	265.5(1)
$c$ / pm	391.1(3)
$c/a$	1.47
Copper position	$0, 0, 0$
Nitrogen position	$1/2, 1/2, 0$
Site occupancy factor of N	0.33(1)

[a] Synchrotron data (ESRF, ID 09A,  $\lambda = 41.3082$  pm)

[b] Ambient pressure:  $a = 381.48(9)$  pm

[c] Time of flight data of the white spallation source at Rutherford Appleton Laboratory, Pearl diffractometer

Table 2. Comparison between experimentally and theoretically obtained properties of LP- $\text{Cu}_3\text{N}$  and the proposed tetragonal high-pressure structure.

lattice constants	$\text{ReO}_3$ type			HP- $\text{Cu}_3\text{N}$		Experiment (8.7/8.2 GPa)
	Experiment (0 GPa)	$p = 0$ GPa	$p = 8.2$ GPa	$p = 0$ GPa	$p = 8.2$ GPa	
$a$ (Å)	3.807(4) [1]	3.84	3.77	2.81	2.76	2.6588/2.655(1)
$c$ (Å)	-	-	-	3.95	3.87	3.9469/3.911(3)
$c/a$	-	-	-	1.41	1.40	1.50/1.47
$V$ (Å <sup>3</sup> /f.u.)	55.18	56.6	53.5	46.9	44.5	41.89/41.34
$\Delta H$ (eV/f.u.)	-	0	2.82	0.87	3.21	-

Table 3. Calculated unit cell data and heat of formation with reference to LP- $\text{Cu}_3\text{N}$  for the most promising ordered compounds  $\text{Cu}_3\text{N}$  and  $\text{Cu}_3\text{N}_{1.125}$ .

compound	space group	$a$ (Å)	$c$ (Å)	$c/a$	$V$ (Å <sup>3</sup> )	$\Delta H$ (eV)
$p = 0$ GPa						
$\text{Cu}_{16}\text{N}_6$	$P4_2/mmc$ (131)	3.89	16.60	1.51	47.2	0.36
$\text{Cu}_{12}\text{N}_4$	$P\bar{4}m2$ (115)	3.88	12.27	1.49	46.2	0.39
$p = 8.2$ GPa						
$\text{Cu}_{16}\text{N}_6$	$P4_2/mmc$ (131)	3.71	4.07	1.50	45.0	-0.16
$\text{Cu}_{12}\text{N}_4$	$P\bar{4}m2$ (115)	3.71	3.99	1.47	44.0	-0.12

## Conclusions

With the conversion from the open framework inverse  $\text{ReO}_3$  crystal structure to a Cu-substructure of one of the dense sphere packings we find a transition from a semiconductor dominated by covalent Cu–N bonding to an interstitial metallic nitride. Thus, the high-pressure phase of  $\text{Cu}_3\text{N}$  connects to the binary nitride phases known from the

1 neighboring 3d elements both in crystal structure and  
2 physical properties.

3  
4 Our total energy calculations and high-pressure  
5 investigations support the experimental findings.  
6 Independent of the nitrogen distribution on the octahedral  
7 voids of the Cu sublattice this type is more stable than the  
8 former theoretically discussed promising structure types.  
9 However, for disordered N atoms, the structure relaxes into  
10 a *fcc* structure. Even disordered phases with higher N  
11 contents prefer this pattern. A reason for the tetragonal  
12 distortion cannot be found. For a total agreement with the  
13 experimentally detected transition pressure and lattice  
14 parameters, there is a need for an ordering of the N atoms.  
15 We offer suggestions for possible structures of HP-Cu<sub>3</sub>N,  
16 that fulfill all required properties, but the coordination  
17 polyhedra in these phases are chemically counterintuitive. A  
18 slight nitrogen enrichment that has been considered due to  
19 experimentally detected elemental copper is likewise  
20 advantageous and cannot be fully excluded. To our opinion,  
21 the structure of the copper sublattice in HP-Cu<sub>3</sub>N is  
22 enlightened, but the distribution of the nitrogen remains an  
23 open question.

## 24 25 Experimental Section

### 26 27 Preparation and Characterization

28 Microcrystalline LP-Cu<sub>3</sub>N was prepared from CuF<sub>2</sub> in flowing  
29 ammonia at 270 °C for 5 h. Higher temperatures or longer reaction  
30 times lead to the formation of increasing amounts of elemental  
31 copper indicating that Cu<sub>3</sub>N is a metastable compound at the  
32 synthesis conditions.

33 X-ray powder diffraction was carried out using an Imaging Plate  
34 Guinier Camera (HUBER diffraction, Cu-K $\alpha_1$  and Co-K $\alpha_1$   
35 radiation, 6  $\times$  15 min scans, 8  $^\circ \leq 2\Theta \leq 100$   $^\circ$ ). Refinements of the  
36 cubic lattice parameter by a least-squares procedure results in  $a =$   
37 381.48(9) pm compared to 381.7(1) pm obtained with single  
38 crystals [2] and 380.7(4) pm from microcrystalline powders [1].  
39 Patterns at temperatures between ambient and 20 K were recorded  
40 in the range of 15  $^\circ \leq 2\Theta \leq 90$   $^\circ$  (Cu-K $\alpha_1$ ) to analyze the thermal  
41 expansion of LP-Cu<sub>3</sub>N. No low-temperature phase transition was  
42 observed; the linear expansion coefficient for the investigated  
43 temperature range resulted in  $\alpha = 6.4(3) \times 10^{-6}$  K<sup>-1</sup>.

44 Chemical analyses on O and N were performed using the carrier  
45 gas hot-extraction technique on a LECO analyzer TCH-600. All  
46 values are averages of at least 3 independent measurements.  
47 Chemical analysis of the starting material results in a composition  
48 of Cu<sub>3</sub>N<sub>0.980(7)</sub>O<sub>0.05(2)</sub> ( $w(\text{O}) = 0.40 \pm 0.14$  %,  $w(\text{N}) = 6.68 \pm$   
49 0.05 %).

50 DTA/TG-measurements were performed using a STA 449C  
51 analyzer (flowing oxygen-, argon- or nitrogen-atmosphere,  
52 99.999 %, thermocouple type S, NETZSCH Gerätebau, Selb).  
53 Temperature calibration was obtained using 5 melting standards  
54 in the temperature range of 370 K  $\leq T \leq 770$  K. In pure oxygen  
55 atmosphere Cu<sub>3</sub>N slowly gains weight above 473 K. For a heating  
56 rate of 10 K/min the exothermic oxidation is accelerated at higher  
57 temperatures to be completed at about 650 K with an overall  
58 weight gain of 16.1 % forming pure CuO (calc.: +16.6 %). In  
59 argon- or nitrogen-atmosphere, an exothermic reaction starting at  
60 about 700 K indicates the metastable nature of low-pressure Cu<sub>3</sub>N.  
In accordance with the observed weight loss of -7.0 %, the

decomposition reaction produces pure copper as the exclusive solid  
product (calculated mass difference -6.8 %).

### Ex-situ high-pressure synthesis experiments and characterization

High-pressure conditions are realized with a hydraulic uniaxial  
press. Force redistribution in order to achieve quasi-hydrostatic  
conditions is accomplished by a Walker-type module (two-stage  
assembly with a central octahedral pressure chamber) and  
MgO/Cr<sub>2</sub>O<sub>3</sub> octahedra with an edge length of 14 mm or 18 mm.  
Elevated temperatures are realized by resistive heating of graphite  
tubes containing the sample crucible. Pressure and temperature  
calibration is completed before the experiments by analyzing the  
resistance changes of bismuth and lead [15] and measuring set-ups  
equipped with a thermocouple, respectively. The crucibles girdling  
the sample mixtures are made from hexagonal boron nitride. X-ray  
powder diffraction data and energy dispersive X-ray analysis do  
not give evidence for a reaction of the container with the sample.  
Thus, separation of reaction products and crucible material can be  
achieved easily. A typical high-pressure synthesis requires pressure  
increase for 3 h, holding at the maximal pressure for typically 5 h  
followed by pressure decrease in 10 h. During maximum pressure  
of 9(1) GPa same samples were heated at 500(70) K for 10 min.  
Heated samples are quenched to ambient temperature by  
disconnecting the heating current before decompression.

### In-situ diffraction experiments at high pressures

Copper nitride was ground into a fine powder and placed in steel  
gaskets using a 4:1 methanol/ethanol mixture, argon or helium,  
respectively, as a pressure transmitting medium. High pressures  
were generated by diamond anvil cells and determined by the ruby  
luminescence method. X-ray powder diffraction experiments were  
carried out at the undulator beamline ID 9A of the ESRF, Grenoble.  
During the exposures samples were oscillated by  $\pm 3^\circ$  in order to  
enhance powder statistics. Typical exposure times were two to five  
seconds. The diffraction patterns were collected on an imaging  
plates detector which is positioned at a distance of approximately  
450 mm from the sample. For calibration of wavelength and  
detector distance we used a silicon standard sample. Integration of  
the two-dimensional raw data was performed using the pattern  
integration software image integrator [16]. Peak positions and  
lattice parameters were refined using the computer program  
WinCSD [17].

Neutron diffraction under hydrostatic pressures was performed at  
the High Pressure Facility at the Pearl beamline of the ISIS pulsed-  
neutron source at the Rutherford Appleton Laboratory as time-of-  
flight experiment. High pressure was obtained in a Ni crucible  
using a Paris-Edinburgh cell equipped with standard tungsten  
carbide anvils. Here, a small lead sphere was used as a pressure  
sensor and quasi-hydrostatic pressure conditions were realized with  
methanol as pressure transmitting medium. Earlier diffraction  
experiments in diamond anvil cells (see above) indicated stability  
of Cu<sub>3</sub>N in alcohol (4:1 mixture of methanol and ethanol) up to 30  
GPa. Structure refinements were performed with the program  
system GSAS [18] within the graphical interface EXPGUI [19].

### In-situ optical spectroscopy

Pressure-dependent absorption measurements were performed in  
the infrared and visible frequency range using a Bruker IFS 66v/s  
spectrometer with an infrared microscope (Bruker IRscopeII). The  
measurements were partly carried out at the infrared beamline of

the synchrotron radiation source ANKA (Angströmquelle Karlsruhe). A diamond anvil cell was used for generation of pressures up to 10 GPa and the ruby luminescence method was used for pressure determination. As hydrostatic pressure transmitting medium we used Ar. In order to determine the transmission of  $\text{Cu}_3\text{N}$  under pressure, the intensity  $I_s(\omega)$  of the radiation transmitted by a small amount of the powder sample and the pressure transmitting medium was measured. As reference, the intensity  $I_r(\omega)$  transmitted by the empty diamond anvil cell was used. The transmission was then calculated according to  $T(\omega) = I_s(\omega)/I_r(\omega)$ . The absorption was calculated as  $A = \log_{10}(1/T)$ .

#### Electronic structure calculations

The first-principles electronic-structure calculations of density-functional type were performed using the Vienna *ab-initio* simulation package [20, 21], plane-wave basis sets and ultra-soft pseudopotentials. The exchange-correlation energy was treated in the generalized gradient approximation (GGA) [22]. The plane-wave cutoff energies were chosen to be 500 eV. The Brillouin zone integrations were performed using the scheme of Monkhorst and Pack [23]. Optimized structural models were obtained by relaxing all forces to values below  $10^{-3}$  eV  $\text{\AA}^{-1}$  and stresses below 1 kbar. To examine the structural behavior at high-pressures, all total energies  $E$  were re-calculated under compression and expansion, and the lattice parameters were scaled in steps of 1% from 91 – 105 % of the minimum geometries. The 15  $E - V$  data points can be fitted by the Murnaghan equation of state [24]. From these the enthalpy–pressure curve easily can be deduced by calculating  $p = -\delta E/\delta V$  and  $H = E + pV$ .

#### Acknowledgments

We thank Dr. Raúl Cardoso for the collection of the ambient pressure X-ray powder diffraction data, Susann Leipe and Dr. Peter Höhn for experimental support, Anja Völzke for performing the chemical analyses, Susann Müller for the operating of the thermal analysis, and Prof. Yuri Grin for valuable discussions. Additionally we wish to acknowledge the assignment of beamtime at the ISIS pearl high-pressure facility and at the undulator beamline ID 9A of the ESRF. We acknowledge the ANKA Angströmquelle Karlsruhe for the provision of beamtime and we would like to thank D. Moss, Y.-L. Mathis, B. Gasharova, and M. Süpfle for assistance using beamline ANKA-IR. This work was supported by the Max-Planck-Gesellschaft and within the Schwerpunktprogramm ‘‘Synthesis, ‘in situ’ characterisation and quantum mechanical modelling of Earth Materials, oxides, carbides and nitrides at extremely high pressures and temperatures’’ of the Deutsche Forschungsgemeinschaft (SPP 1236). Financial support by the Deutsche Forschungsgemeinschaft through the Emmy Noether-program and the SFB 484 is gratefully acknowledged.

- [1] R. Juza, H. Hahn, *Z. Anorg. Allg. Chem.* **1938**, 239, 282–287.
- [2] U. Zachwieja, H. Jacobs, *J. Less-Common Met.* **1990**, 161, 175–184.
- [3] J. E. Jorgensen, W. G. Marshall, R. I. Smith, J. S. Olsen, L. Gerward, *J. Appl. Crystallogr.* **2004**, 37, 857–861 and references therein.
- [4] Z. Cancarevic, J. C. Schön, M. Jansen, *Z. Anorg. Allg. Chem.* **2005**, 631, 1167–1171.
- [5] W. Yu, L. Li, C. Jin, *J. Mater. Sci.* **2005**, 40, 4661–4664.
- [6] L. X. Yang, J. G. Zhao, Y. Yu, F. Y. Li, R. C. Yu, C. Q. Jin, *Chin. Phys. Lett.* **2006**, 23, 426–427.

- [7] J. G. Zhao, L. X. Yang, Y. Yu, S. J. You, J. Liu, C. Q. Jin, *phys. Stat. sol (b)* **2006**, 243, 573–578.
- [8] a) P. W. Stephens, *J. Appl. Cryst.* **1999**, 32, 281–289; b) R. E. Dinnebier, R. Von Dreele, P. W. Stephens, S. Jelonek, J. Sieler, *J. Appl. Cryst.* **1999**, 32, 761–769.
- [9] A. Leinweber, R. Niewa, H. Jacobs, W. Kockelmann, *J. Mater Chem.* **2000**, 10, 2827–2834.
- [10] L. M. Corliss, N. Elliott, J. M. Hastings, *Phys. Rev.* **1960**, 117, 929–935.
- [11] J.-E. Jørgensen, J. Staun Olsen, L. Gerward, *J. Appl. Cryst.* **2000**, 33, 279–284.
- [12] Ma. Guadalupe Moreno-Armenta, W. López Pérez, N. Takeuchi, *Solid State Sci.* **2007**, 9, 166–172.
- [13] N. Matsuno, M. Yoshimi, S. Ohtake, T. Akahane, N. Tsuda, *J. Phys. Soc. Jpn.* **1978**, 45, 1542–1544.
- [14] U. Hahn, W. Weber, *Phys. Rev. B* **1996**, 53, 12684–12693.
- [15] D. A. Young, *Phase diagram of the elements*, University of California Press, Berkeley 1991.
- [16] L. Akselrud, *Image Integrator*, Version 1.2, Max-Planck-Institut für Chemische Physik fester Stoffe, Dresden, **2005**.
- [17] L. G. Akselrud, P. Y. Zavalii, Yu. N. Grin, V. K. Pecharsky, B. Baumgartner, E. Woelfel, *Materials Science Forum* **1993**, 133–136, 335–340.
- [18] A. C. Larson, R. B. Von Dreele, *General Structure Analysis System (GSAS)*, Los Alamos National Laboratory Report **2004**, 86-748.
- [19] B. H. Toby, *J. Appl. Cryst.* **2001**, 34, 210–213.
- [20] G. Kresse, J. Hafner, *Phys. Rev. B* **1993**, 47, 558–561; *Phys. Rev. B* **1994**, 49, 14251–14269.
- [21] G. Kresse, J. Furthmüller, *Comput. Mat. Sci.* **1996**, 6, 15–50; *Phys. Rev. B* **1996**, 55, 11169–11186.
- [22] J. P. Perdew, in: *Electronic Structure of Solids ’91* (Eds.: P. Ziesche H. Eschrig), Akademie Verlag, Berlin, **1991**, page 11.
- [23] H. J. Monkhorst, J. D. Pack, *Phys. Rev. B* **1976**, 13, 5188–5192.
- [24] F. D. Murnaghan, *Prog. Natl. Acad. Sci. USA* **1944**, 30, 244–247.

Received: ((will be filled in by the editorial staff))  
Published online: ((will be filled in by the editorial staff))

1  
2  
3  
4  
5  
6  
7  
8  
9  
10  
11  
12  
13  
14  
15  
16  
17  
18  
19  
20  
21  
22  
23  
24  
25  
26  
27  
28  
29  
30  
31  
32  
33  
34  
35  
36  
37  
38  
39  
40  
41  
42  
43  
44  
45  
46  
47  
48  
49  
50  
51  
52  
53  
54  
55  
56  
57  
58  
59  
60

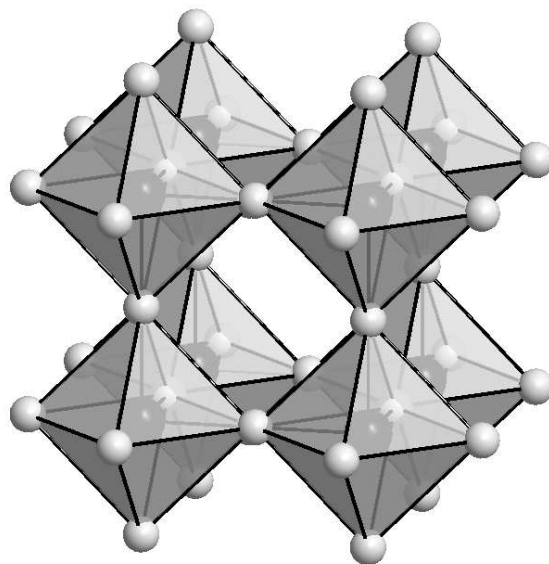


Figure 1. Crystal structure of the low-pressure modification of  $\text{Cu}_3\text{N}$  ( $\text{ReO}_3$  type). White spheres correspond to copper atoms, the vertex-sharing coordination octahedra surrounding nitrogen are indicated.

285x178mm (96 x 96 DPI)

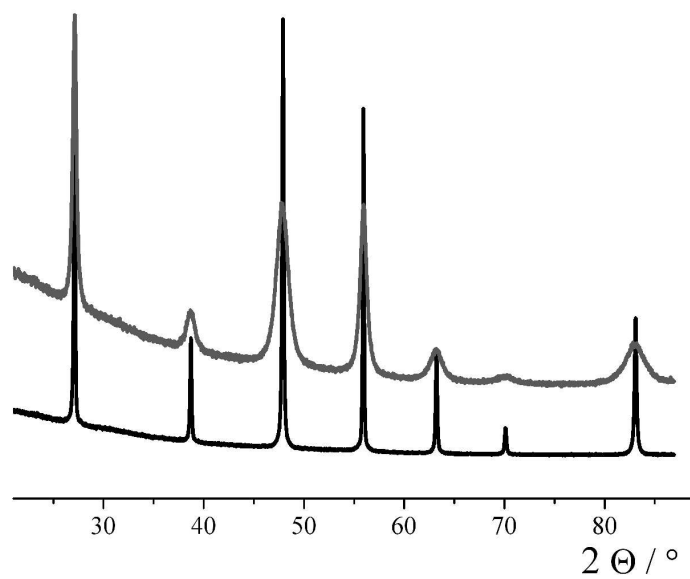
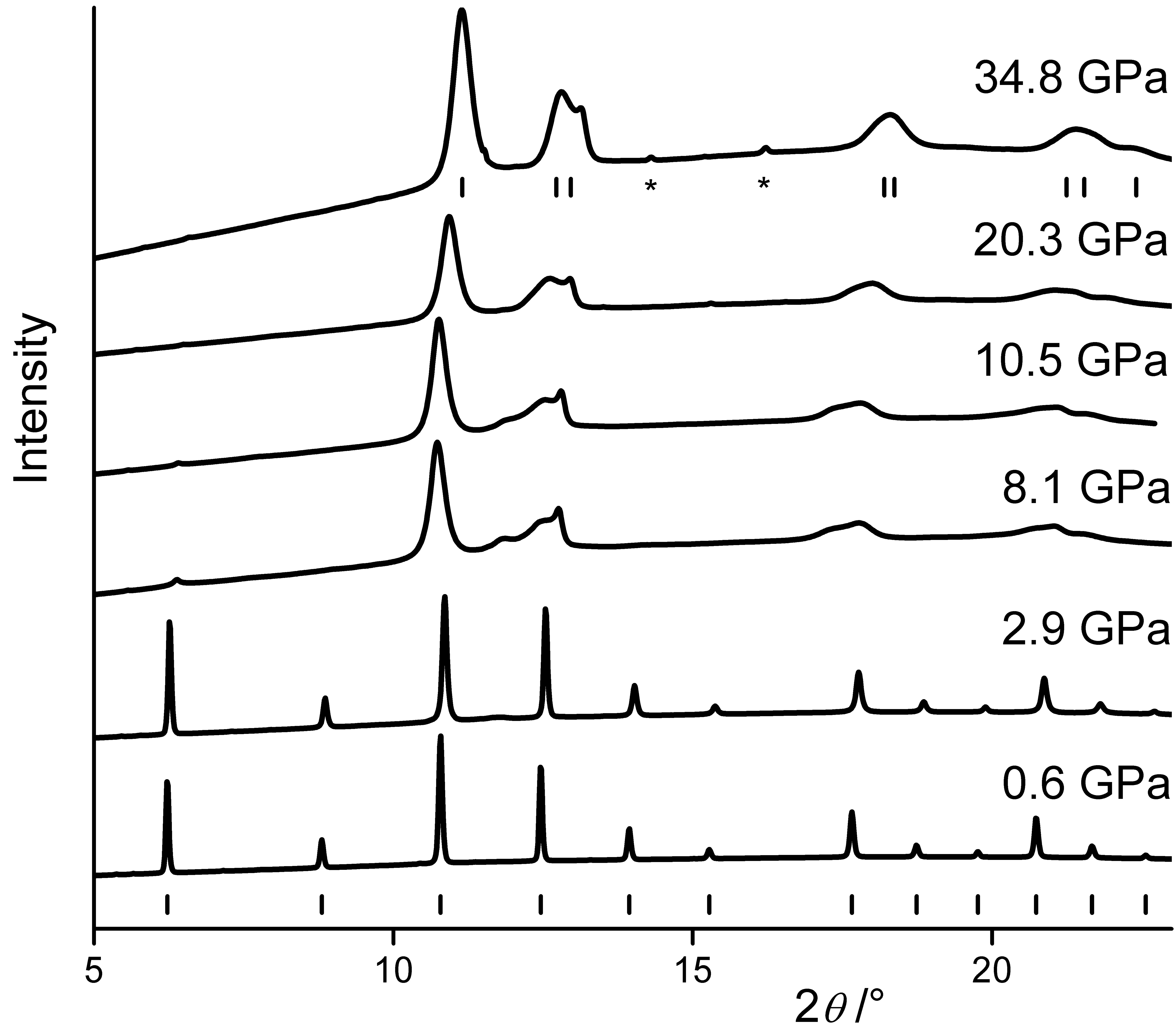
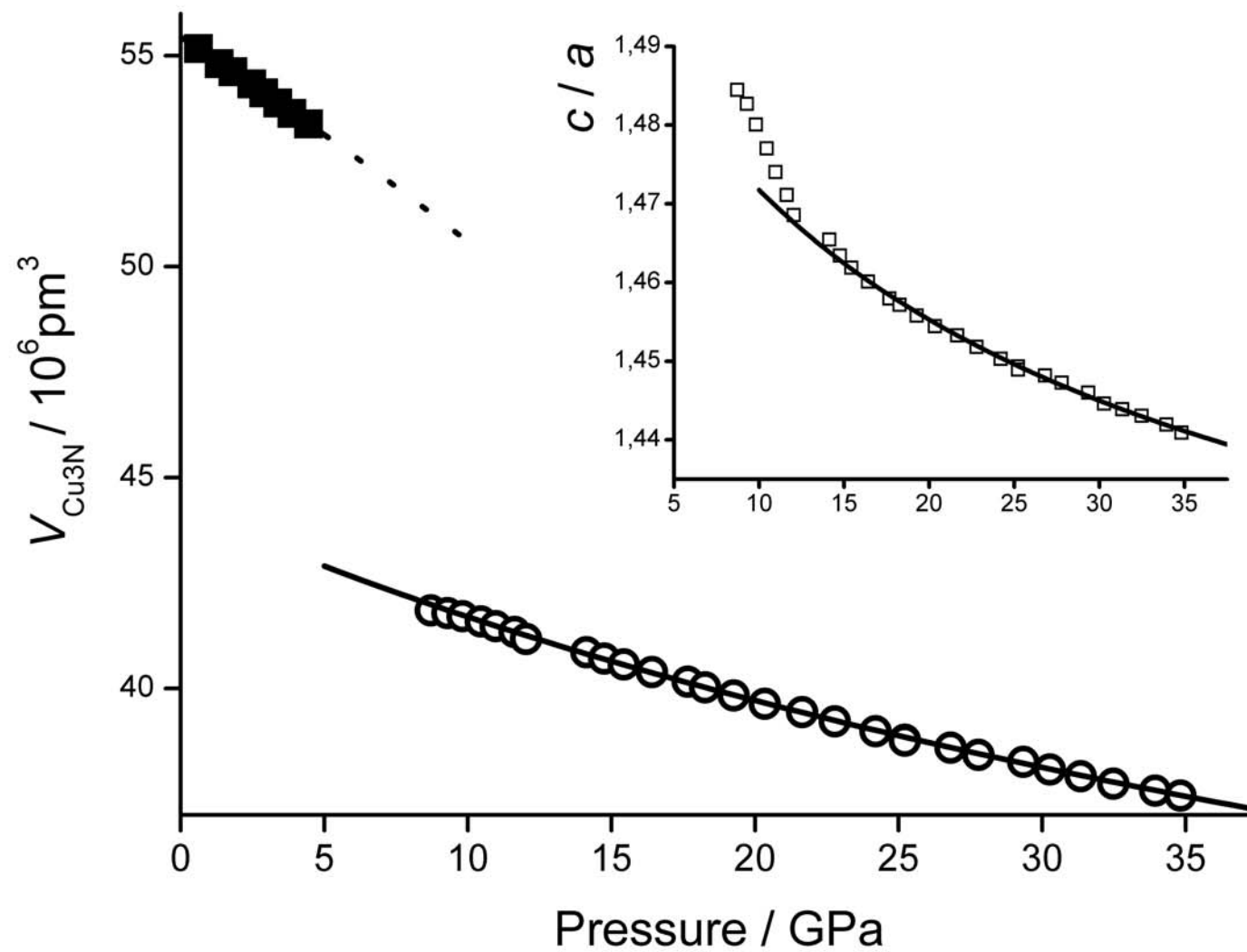
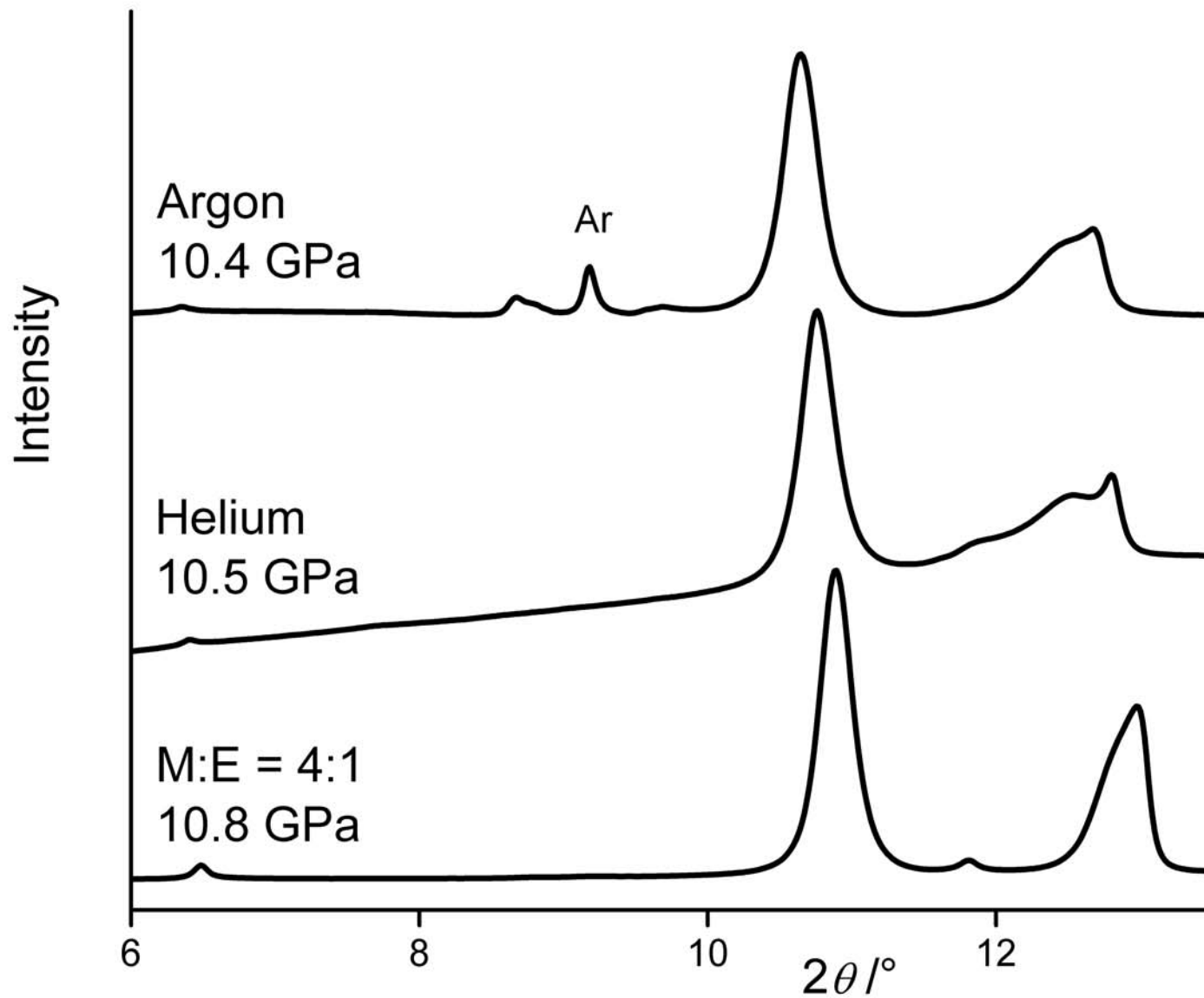


Figure 2. XRD pattern of LP-Cu<sub>3</sub>N before (bottom line) and after (top line) a pressure treatment in the multi-anvil cell at about 9 GPa (Co-K $\alpha$ 1 radiation).  
594x419mm (150 x 150 DPI)

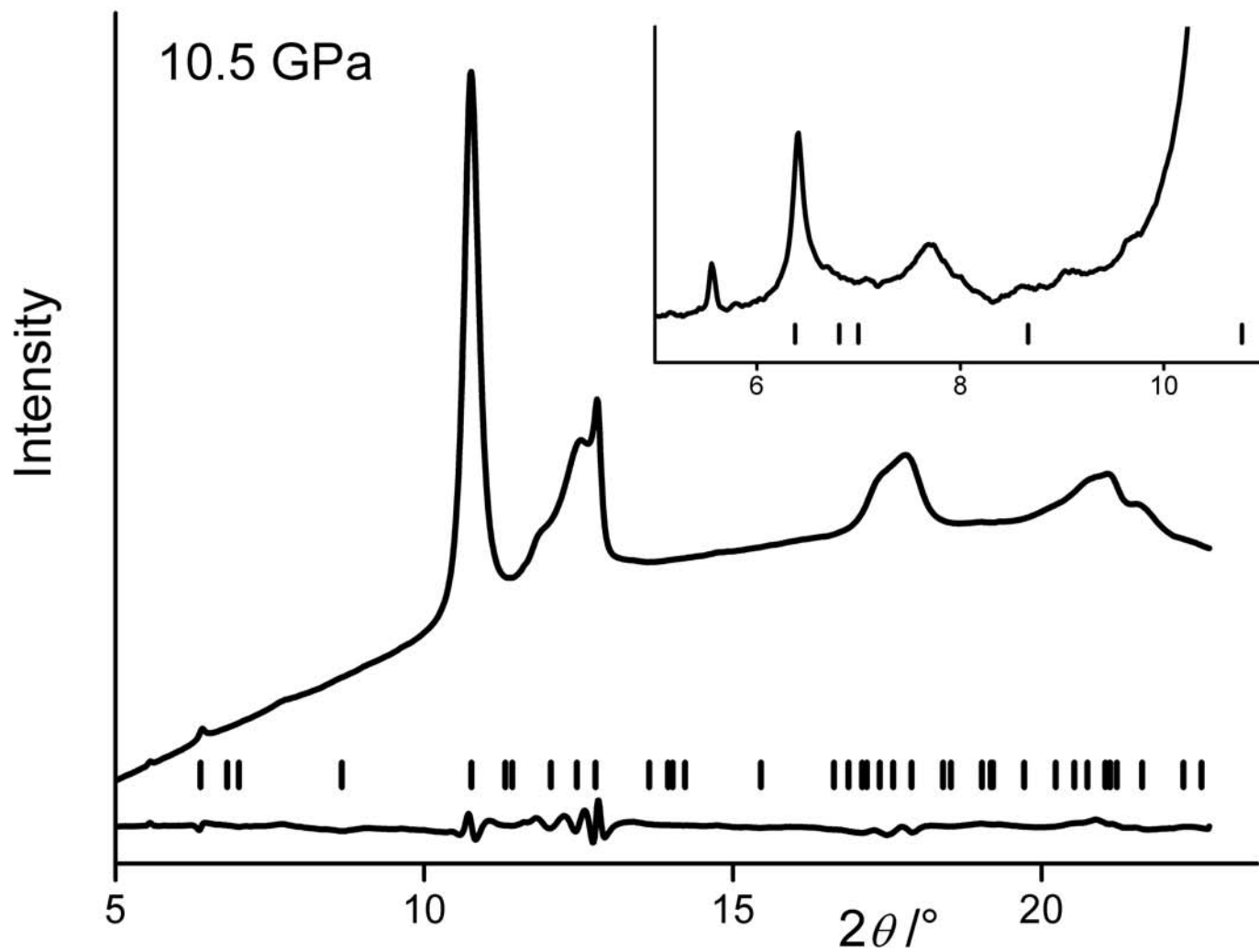
1  
2  
3  
4  
5  
6  
7  
8  
9  
10  
11  
12  
13  
14  
15  
16  
17  
18  
19  
20  
21  
22  
23  
24  
25  
26  
27  
28  
29  
30  
31  
32  
33  
34  
35  
36  
37  
38  
39  
40  
41  
42  
43  
44  
45  
46  
47  
48  
49  
50  
51  
52  
53  
54  
55  
56  
57  
58  
59  
60







1  
2  
3  
4  
5  
6  
7  
8  
9  
10  
11  
12  
13  
14  
15  
16  
17  
18  
19  
20  
21  
22  
23  
24  
25  
26  
27  
28  
29  
30  
31  
32  
33  
34  
35  
36  
37  
38  
39  
40  
41  
42  
43  
44  
45  
46  
47



1  
2  
3  
4  
5  
6  
7  
8  
9  
10  
11  
12  
13  
14  
15  
16  
17  
18  
19  
20  
21  
22  
23  
24  
25  
26  
27  
28  
29  
30  
31  
32  
33  
34  
35  
36  
37  
38  
39  
40  
41  
42  
43  
44  
45  
46  
47

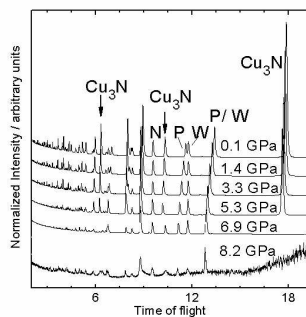


Figure 7. Neutron diffraction patterns (TOF in  $\mu\text{s}$ ) of  $\text{Cu}_3\text{N}$  measured at different pressures. N, P and W assign prominent reflections of Ni crucible, lead pressure indicator and WC anvils, respectively.  
288x200mm (150 x 150 DPI)

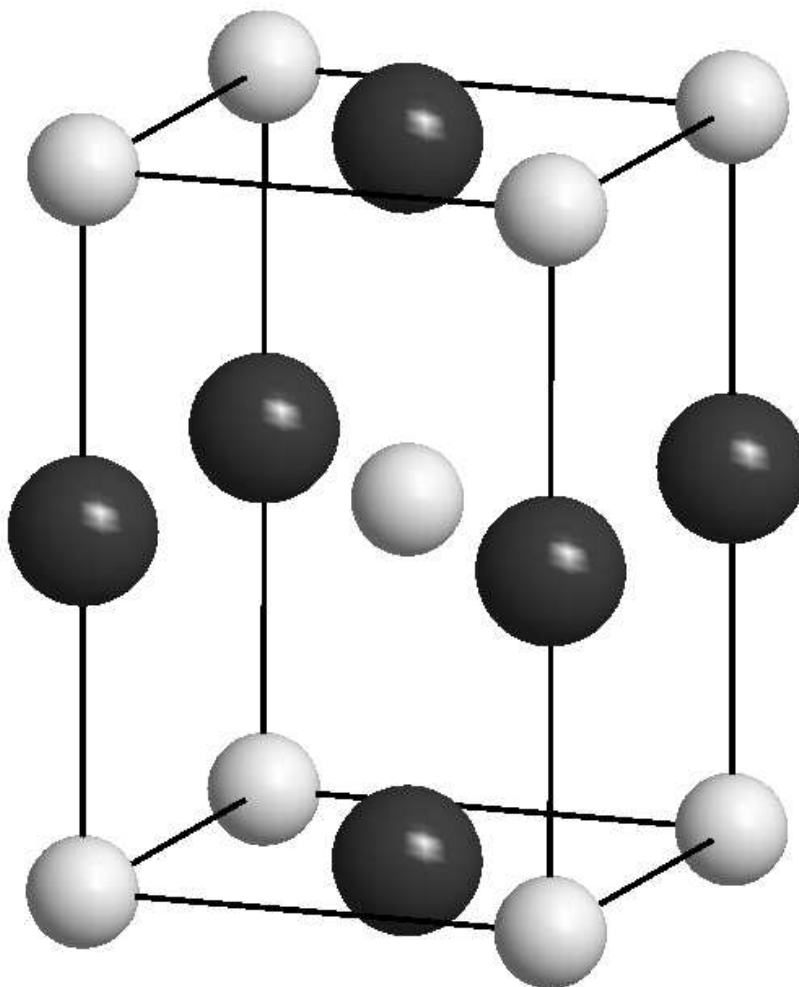


Figure 8. Average tetragonal crystal structure of the high-pressure modification of Cu<sub>3</sub>N from experimental data. White spheres correspond to copper atoms. Nitrogen positions (dark spheres) are only occupied to  $\frac{1}{3}$ <sup>rd</sup>.  
162x178mm (96 x 96 DPI)

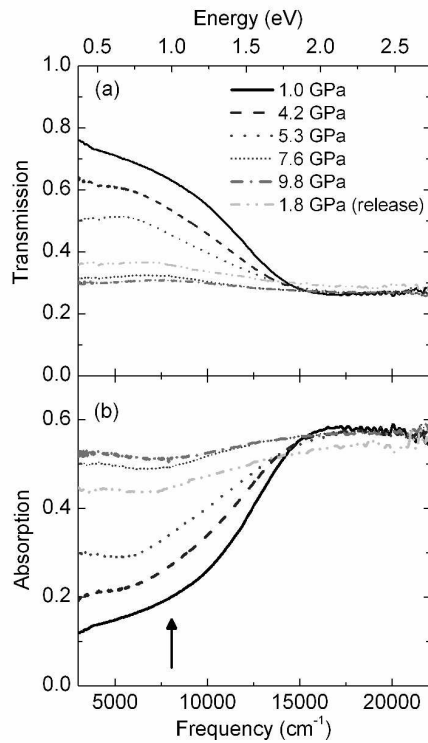
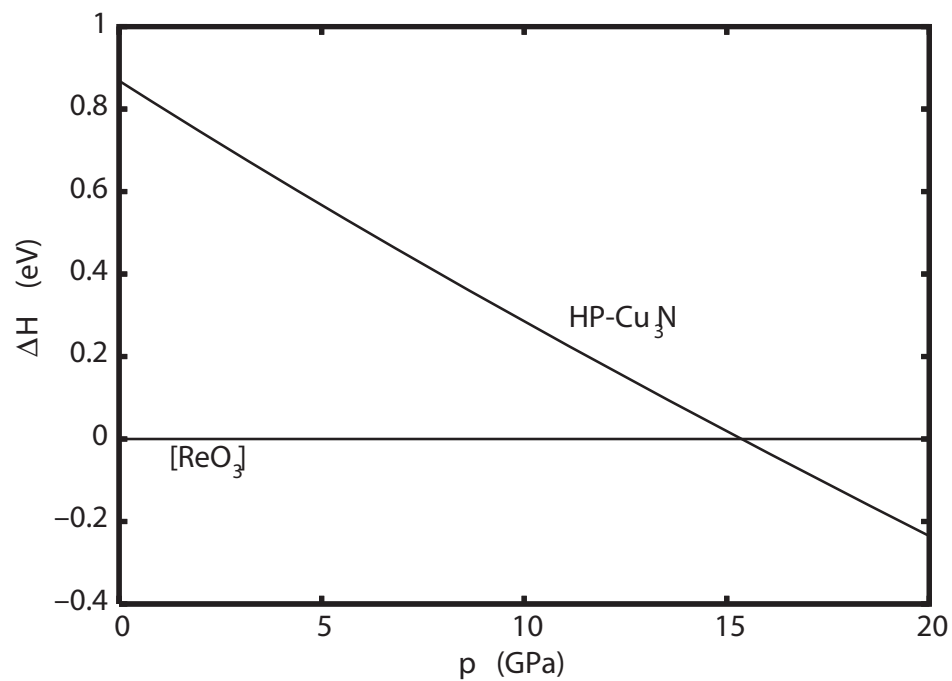
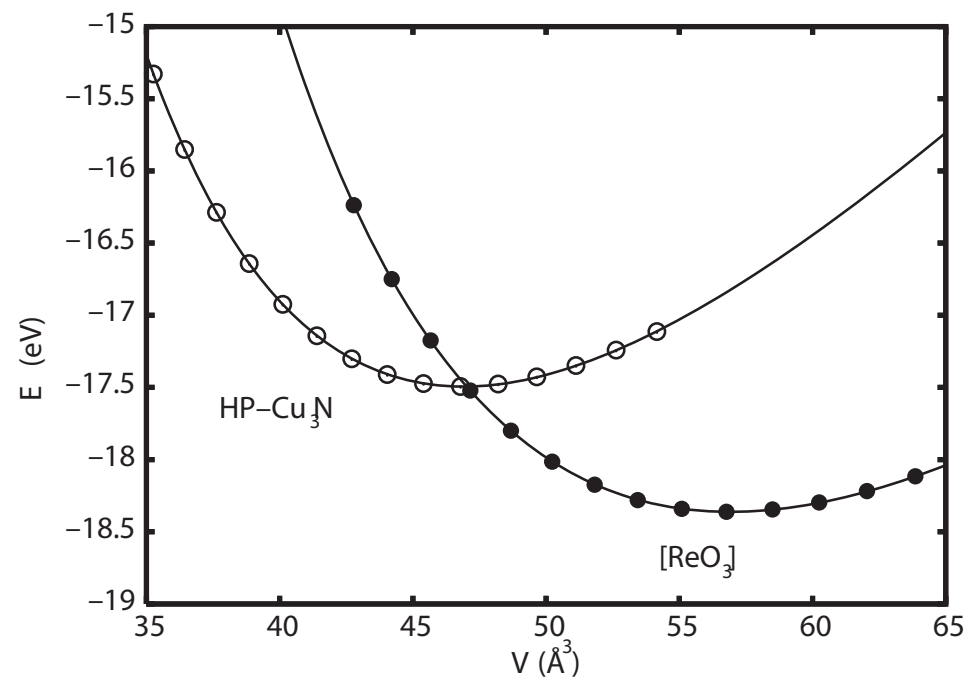
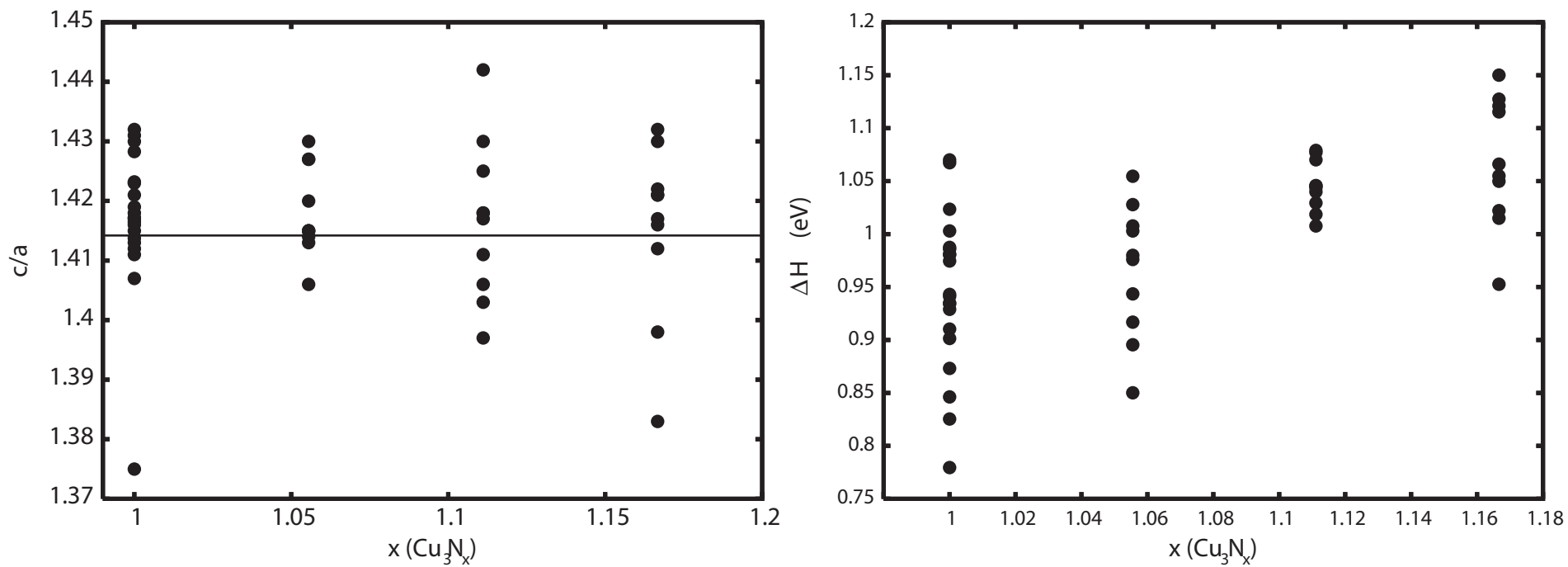
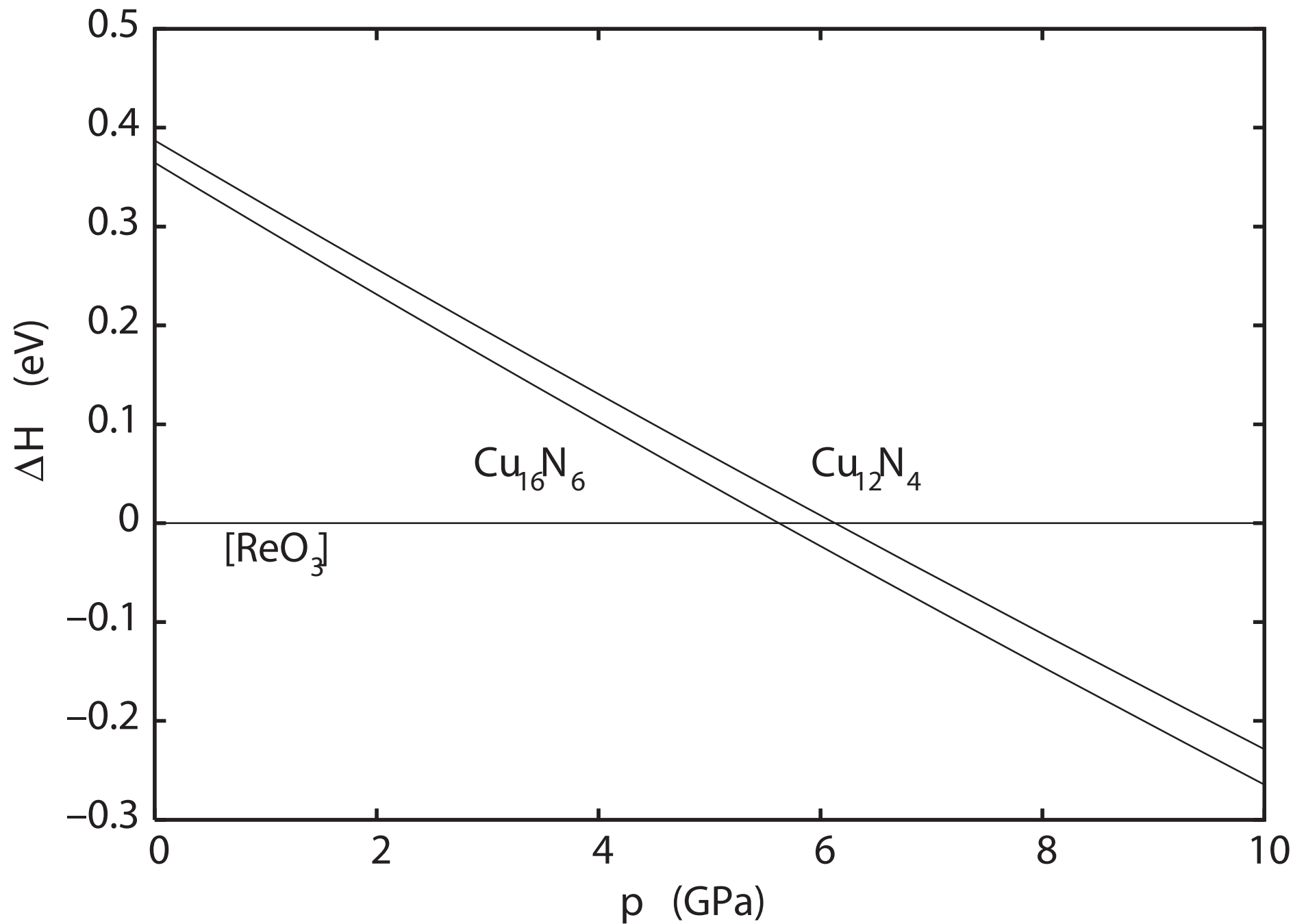


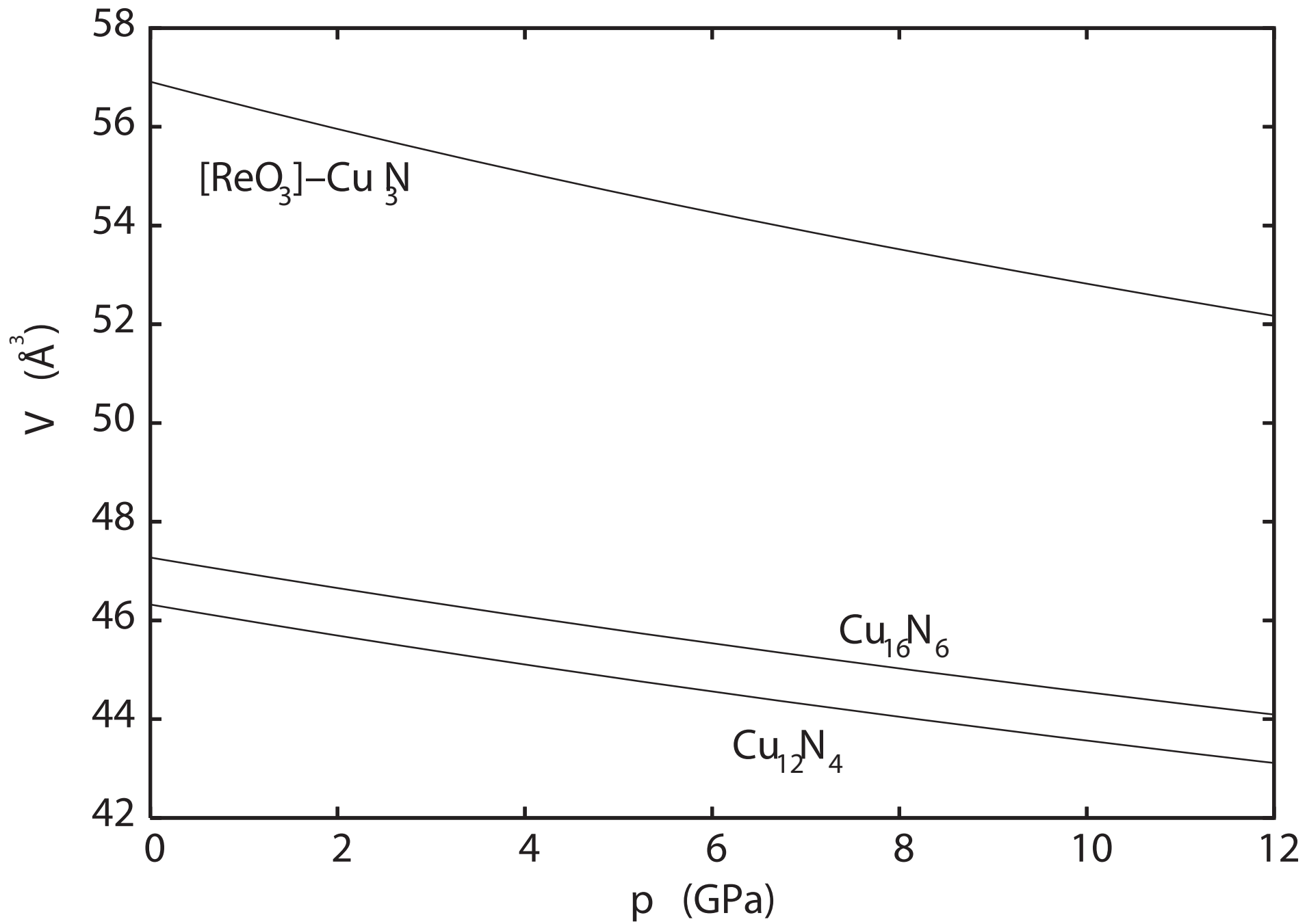
Figure 9. (a) Transmission  $T(\omega) = I_s(\omega)/I_r(\omega)$  (see text for definitions) of  $\text{Cu}_3\text{N}$  at ambient temperature as a function of pressure and (b) the corresponding absorption  $A = \log_{10}(1/T)$  as a function of pressure. The arrow in (b) indicates the frequency position of the absorption edge.  
558x431mm (150 x 150 DPI)



1  
2  
3  
4  
5  
6  
7  
8  
9  
10  
11  
12  
13  
14  
15  
16  
17  
18  
19  
20  
21  
22  
23  
24  
25  
26  
27  
28  
29  
30  
31  
32  
33  
34  
35  
36  
37  
38  
39  
40  
41  
42  
43  
44  
45  
46  
47



1  
2  
3  
4  
5  
6  
7  
8  
9  
10  
11  
12  
13  
14  
15  
16  
17  
18  
19  
20  
21  
22  
23  
24  
25  
26  
27  
28  
29  
30  
31  
32  
33  
34  
35  
36  
37  
38  
39  
40  
41  
42  
43  
44  
45  
46  
47



1  
2  
3  
4  
5  
6  
7  
8  
9  
10  
11  
12  
13  
14  
15  
16  
17  
18  
19  
20  
21  
22  
23  
24  
25  
26  
27  
28  
29  
30  
31  
32  
33  
34  
35  
36  
37  
38  
39  
40  
41  
42  
43  
44  
45  
46  
47

